Ecological Indicators 79 (2017) 173–181

Contents lists available at ScienceDirect

Ecological Indicators

journal homepage: www.elsevier.com/locate/ecolind

Original Articles

Development of remote sensing indicators for mapping episodic die-off of an invasive annual grass (*Bromus tectorum*) from the Landsat archive

Peter J. Weisberg[a,*], Thomas E. Dilts[a], Owen W. Baughman[a], Susan E. Meyer[b], Elizabeth A. Leger[a], K. Jane Van Gunst[a,1], Lauren Cleeves[a,2]

[a] Department of Natural Resources and Environmental Science, University of Nevada, Reno, NV, 89557 USA
[b] U.S. Forest Service Rocky Mountain Research Station, Shrub Sciences Laboratory, 735 North 500 East, Provo, UT, 84606, USA

ARTICLE INFO

Keywords:
Remote sensing
Seed pathogens
Invasive plants
Great Basin
Cheatgrass
Landscape pathology

ABSTRACT

The exotic annual grass *Bromus tectorum* (cheatgrass) dominates vast acreages of rangeland in the western USA, leading to increased fire frequency and ecosystem degradation that is often irreversible. Episodic regeneration failure ("die-off") has been observed in cheatgrass monocultures and can have negative ecosystem consequences, but can also provide an opportunity for restoration of native species and ecological function within the imperiled sagebrush steppe ecosystem. Proximate causes of cheatgrass die-off are uncertain, although several taxa of fungal soil pathogens have been implicated. Die-off occurrence is stochastic and can occur in remote areas. Thus, developing remote sensing indicators that are repeatable over long time periods, across extensive regions, and at relatively fine spatial resolution would be beneficial for accurately pinpointing events.

We developed a remote sensing approach for mapping historical die-off from the Landsat archive (1985–2015), and used this to quantify spatial and temporal patterns of die-off occurrence annually at 30-m resolution. A Random Forests classification of image-derived spectral endmembers, trained on 2014 data, predicted die-off with 93% accuracy ($\kappa = 0.845$) when applied to independent validation data from 2009. Die-off extent varied greatly across years, though some areas experienced die-off multiple times during the observation period. We found a strong correspondence between die-off occurrence and winter drought conditions, with strongest negative associations with current-year winter precipitation and previous years' lagged winter and annual precipitation. Die-off duration was heavily skewed towards single-year die-off (81.5% of events), even in localized areas of more frequent occurrence ('die-off hotspots').

Our retrospective classification of the Landsat archive suggests that cheatgrass die-off occurrence is predictable as the intersection of particular site environmental conditions with annual weather conditions, possibly because they are favorable for disease expression. Associations with previous year conditions suggest that die-off may also depend upon feedbacks between cheatgrass dominance and litter production, suitable sites for seedling establishment, and abundance and persistence of pathogen inoculum. Remote sensing indicators such as those developed in this study are needed to develop hypotheses about die-off causal factors, as well as support improved management of cheatgrass, mitigation for negative consequences associated with die-off (e.g. wind erosion), and successful restoration of native plant communities on die-off areas.

1. Introduction

The spread of the exotic winter annual grass *Bromus tectorum* L. (cheatgrass, downy brome) throughout the western United States has been transformative since its initial introduction in the late 1880s (Mack, 1981). Invasion of cheatgrass into shrub-dominated vegetation types increases fine fuel continuity and facilitates more frequent wildfires (Balch et al., 2013), as a regional manifestation of the grass-fire cycle that affects rangeland ecosystems globally (D'Antonio and Vitousek, 1992). Increased fire frequencies and earlier fire seasonality favor this invasive species over fire-intolerant native shrubs such as big sagebrush (*Artemisia tridentata* Nutt.) which require longer fire-free intervals for maturation and seed production (Young and Evans 1978). Seedlings of native shrubs, grasses and forbs are typically not compe-

* Corresponding author at: Department of Natural Resources and Environmental Science, University of Nevada, Reno, 1664 N. Virginia St., Reno, NV, 89557, USA.
E-mail address: pweisberg@cabnr.unr.edu (P.J. Weisberg).
[1] Present address: Nevada Department of Wildlife, 815 E. Fourth Street, Winnemucca, NV, 89445, USA.
[2] Present address: U.S. Geological Survey, 970 Lusk Street, Boise, ID, 83706, USA.

http://dx.doi.org/10.1016/j.ecolind.2017.04.024
Received 4 September 2016; Received in revised form 25 March 2017; Accepted 10 April 2017

titive with cheatgrass in dry-summer climates, greatly impeding natural recovery (Humphrey and Schupp, 2004; Rafferty and Young, 2002; Rowe and Leger, 2011). The outcomes of these processes are often highly altered plant communities, altered fire regimes and increased dominance of the annual grass component, with associated ecological degradation and loss of rangeland productivity (D'Antonio and Vitousek, 1992). It is arguable that cheatgrass invasion, along with concomitant alterations to land cover, habitat, resources, disturbance regime, and ecosystem services, comprises the single most damaging exotic plant invasion in the western United States (Duncan et al., 2004).

A commonly observed but poorly studied phenomenon in cheatgrass monocultures is the intermittent occurrence of 'die-off' or stand failure, where a cheatgrass stand fails to re-establish or is destroyed prior to seed production, despite receiving adequate precipitation for establishment (Baughman et al., 2016; Blank et al., 2011; Meyer et al., 2014). Cheatgrass die-offs occur at multiple spatial scales and in contrasting ecological settings, suggesting that there may be multiple causal agents, both abiotic and biotic, and that these agents may interact in complex ways to produce the die-off effect. While the proximate mechanisms underlying cheatgrass die-off have yet to be determined, recent studies have identified several fungal pathogens found in die-off patches that can produce cheatgrass die-off failure under controlled laboratory conditions (Meyer et al., 2014). Die-offs sometimes occur over very large areas and can have negative consequences, including increased soil erosion and desertification, loss of forage for livestock and wildlife, and invasion by secondary perennial weeds. However, cheatgrass die-off can also provide a restoration opportunity (Baughman et al., 2016). This might be especially so in die-offs that occur in the same area for multiple years, as the prolonged reduction in competition could result in significantly increased native plant performance (Baughman and Leger, pers. obs).

Cheatgrass die-off has been observed to occur more frequently in certain areas than in others (Baughman et al., 2016), but occurrence is highly stochastic and often in remote areas. On-the-ground detection of cheatgrass die-off is therefore unreliable and inconsistent, and remote sensing indicators are sorely needed to quantify die-off incidence over long time periods and across extensive regions. Remote sensing methods could lead to new insights on die-off causes, or new predictive capacity to forecast future die-off occurrence, if they have sufficient spatial resolution and are repeatable over long time periods, allowing quantification of die-off extent, duration, periodicity, and correlation with site conditions and annual weather variability.

Because of the importance of this phenomenon, other methods have been developed to observe cheatgrass die-offs. An existing approach to mapping cheatgrass die-off (Boyte et al., 2015) first uses coarse-resolution (250-m) MODIS data to develop a "cheatgrass index" based on the difference between spring and summer greenness, then models expected cheatgrass performance statistically using bioclimatic variables, and finally predicts die-off as pixels with highly negative deviations from the statistical model. The resulting products are valuable for understanding die-off occurrence over broad regions, but the coarse resolution limits utility for rangeland management decisions, particularly in areas where die-off patches tend to be small, spatially heterogeneous and with shifting boundaries from year to year. Also, models of cheatgrass cover based upon intra-annual phenology (e.g. Boyte et al., 2015; Peterson, 2005; Singh and Glenn, 2009) can be error-prone because cheatgrass often co-occurs with other ruderal species that have contrasting, late-season phenology, masking the expected signal for this early season species. This highlights a potential problem with the approach of assessing cheatgrass die-off as high deviance from model predictions, as the robustness of the classification relies upon developing highly accurate cheatgrass cover models, incorporating cheatgrass cover model uncertainty within the classification error.

Here, our goal was to develop a remote sensing method for mapping cheatgrass die-off from readily available (Landsat) imagery at moderate resolution (30-m) suitable for guiding landscape restoration efforts. Our approach differs from previous methods in that it relies solely upon the spectral properties of die-off patches, allowing for a direct classification of cheatgrass die-off occurrence. Specific objectives were to:

(1) Develop a robust remote sensing methodology for classifying cheatgrass die-off that allowed quantification of interannual variability at 30-m resolution across the archival Landsat chronology (1985–2015);
(2) Distinguish single-year die-off events ("transient die-off") from events that persist across years ("persistent die-off"), and distinguish die-off events that occur only once in a location from events that occur more consistently in the same "hotspot" locations over the 30-year period ("hotspot die-off");
(3) Explore climate relationships associated with the area of die-off to occur in a given year, separately for transient and persistent die-off;
(4) Quantify the spatial extent, patch size and duration of die-off events, to inform future field and laboratory studies of die-off causal mechanisms, as well as to help prioritize potential restoration efforts in die-off areas.

Our approach using the Landsat archive facilitates hindcasting of historical cheatgrass die-off over a multi-decadal period, which allows land managers to place current die-off into a long-term context and could lead to statistical models for predicting future die-off. Our approach also allows relatively rapid delineation of current-year die-off, soon after the peak green-up period for cheatgrass in spring. Here, we also discuss the results of our remote sensing findings in relation to field and laboratory research on die-off causal mechanisms, and suggest hypotheses about possible mechanisms from this inferential method.

2. Methods

2.1. Study area

The study area includes the Nevada portion of Landsat scenes (Worldwide Reference System 2: Path 42/Rows 32 and 31) centered on Winnemucca, Nevada; an area that has been subject to extensive cheatgrass invasion, as well as invasion by other exotic annual species such as Russian thistle (*Salsola tragus* L.) and tumble mustard (*Sisymbrium altissimum* L.), which often occur mixed with cheatgrass. The study area was chosen because it is an area where cheatgrass die-offs had been observed in the field (Salo, 2011) and because the long duration of cloud-free Landsat scenes in the spring months made it amenable to the time series analysis. Playas, sand dunes, areas of irrigated agriculture, roads, urban areas, lakes, wetlands, riparian areas, and pinyon juniper woodlands were excluded from the study.

After masking out higher elevations that were dominated by trees or montane shrub communities, elevations of pixels considered in the analysis ranged from 1163 to 2031 m above sea level, with an average elevation of 1465 m. The climate of the study area can be characterized as arid cold desert with an average January minimum temperature of −7 °C and an average July maximum temperature of 32 °C. Average annual precipitation was 251 mm, but precipitation is highly variable from year to year (30-year range: 110–711 mm; PRISM Climate Group, 2014). Prior to conversion to cheatgrass due to frequent wildfire, the majority of the study area was dominated by Wyoming big sagebrush (*Artemisia tridentata* Nutt. ssp. *wyomingensis* Beetle & Young), but some of the lowest elevation portions of the study area are salt desert shrubland dominated by species such as winterfat (*Krascheninnikovia lanata* (Pursh) A. Meeuse & Smit) and shadscale (*Atriplex confertifolia* (Torr. & Frém.) S. Watson).

2.2. Image processing

Fifty-two Landsat Thematic Mapper (TM) images, two Landsat Thematic Mapper (ETM+) images (2012), and six Landsat

Operational Land Imager (OLI) images (2013–2015) (Worldwide Reference System2: Path 42/Rows 32 and 31) were downloaded from the USGS GLOVIS website (http://glovis.usgs.gov). The images chosen represent a balance between the need to minimize cloud cover and acquire dates that are as close as possible to peak greenness of cheatgrass which occurs during April and May in our study area (Supplementary materials: Table S1). The period of image acquisition ranged from March 18th to June 28th, with 90% of images falling between April 2nd and May 26th. Suitable images were found for all years within the 1985–2015 period of study except for 2011, where Landsat image collections coincided with cloudy springtime conditions in the study area. Therefore, the year 2011 is excluded from our analysis.

Images were first converted to top-of-atmosphere reflectance and carefully preprocessed to remove clouds, cloud shadows, and areas of snow cover. Images were converted to at-sensor radiance using the spectral radiance scaling method (Chander et al., 2009) and then converted to top-of-atmosphere reflectance using the CHKUR solar spectrum of MODTRAN 4.0 for Landsat TM and the reflectance rescaling coefficients in the Landsat 8 metadata files. The thermal bands for all Landsat sensors and the coastal blue band of Landsat 8 were excluded from further analysis. Images had clouds, cloud shadows, and snow removed using fMask software (Zhu et al., 2012). Default settings were used and the resulting masks showed good performance when evaluated visually. Masked areas were removed from all subsequent analysis steps.

The study area is characterized by rugged topography. Although all images obtained were at the L1T level of geometric and terrain correction, we further corrected for topographic shadowing and differential illumination by using the statistical-empirical correction method of Meyer et al. (1993) as implemented in Greenwood and Weisberg (2009). A hillshade was generated using a digital elevation model with the altitude and azimuth parameters derived from the Landsat metadata file. We regressed the topographic hillshade image on the brightness values for each band. The hillshade was then multiplied by the slope value from the regression, and the intercept value was added to the result to produce an image of the terrain-induced illumination. We subtracted this image from each Landsat band and added the mean brightness value from the original Landsat band. The six bands were composited to produce a multispectral image estimating the reflectance in the absence of topographic variation.

Radiometric normalization among multiple Landsat scenes was accomplished using linear regression prior to mosaicking, to achieve a single seamless image with comparable spectral properties. For each year, Path 42 Row 32 was processed as the reference image with Path 42 Row 31 adjusted to match. Overlapping pixels were identified and linear regression was used to determine the relationship between brightness values for the two images. Predicted brightness values were then applied to the normalized image, after which images were mosaicked using a feathering algorithm (“blend” option) in ArcGIS 10.1 software (Esri, 2012).

2.3. Cheatgrass die-off classification and validation

We first conducted spectral mixture analysis (SMA), a remote sensing approach that mathematically models pixels as compositional mixtures of dominant, but spectrally distinct features (i.e., endmembers), to derive fractional cover of key vegetation components. We then used a machine learning algorithm to predict the probability of cheatgrass die-off within each pixel according to the fractional covers from SMA. Cheatgrass die-off events were classified on a per-pixel basis using a hard classification based on threshold die-off probability values derived from training sites collected in the field.

Recent studies have shown that spectral mixture analysis can improve vegetation cover mapping in arid and semi-arid regions compared to methods that use vegetation indices (Bradley and Fleishman, 2008; Elmore et al., 2000; Yang et al., 2012). Using SMA, we derived the following four fractional cover maps: photosynthetic vegetation (PV), non- photosynthetic vegetation (NPV), soil, and shade. We used image-derived endmembers rather than laboratory spectra following the approach of Yang et al. (2012). Endmembers were identified using the SMACC (Sequential Maximum Angle Convex Cone) tool in ENVI 4.8 (Exelis Visual Information Solutions, 2012). To ensure that the endmembers represented features common to desert rangelands and most pertinent to the objectives of our cheatgrass die-off study, a subset of the study area free of agriculture, urbanization, and wetlands was used and endmembers were examined with 1-m National Agriculture Inventory Imagery (NAIP). We did not perform shade normalization, but retained the original fractional values of all four endmembers (Fig. 1).

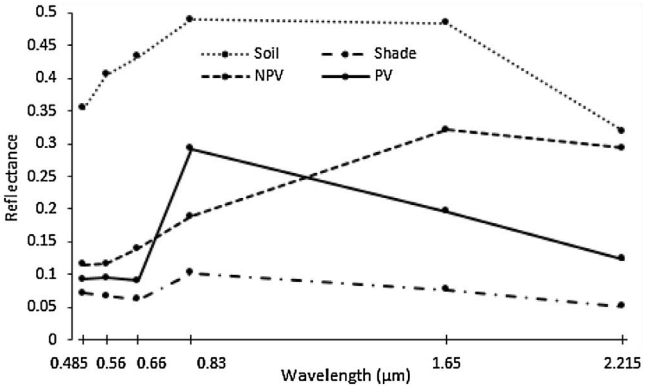

Fig. 1. Image-derived reflectance characteristics of the four endmembers based on Landsat TM: PV = photosynthetic vegetation; NPV = non-photosynthetic vegetation.

A combination of field sampling and manual interpretation of Landsat imagery was used to generate training data for cheatgrass monoculture and cheatgrass die-off cover types in the year 2014. Die-off areas and adjacent non-die-off control areas were first field-mapped using high-precision GPS. Spectral properties of field-mapped die-off areas were used to photo-interpret 180 die-off polygons from both WRS 42/32 and WRS 42/31 that could be identified visually from Landsat imagery using a false-color composite of the near-infrared, red, and green channels. The photo-interpreted polygons were then used to generate 471 random “die-off” points. An additional 1382 random points were generated in areas within 250 m but outside of the photo-interpreted die-off polygons. Non-die-off points were visually checked and questionable observations were deleted.

Spectral endmembers that best distinguished die-off from cheatgrass and shrub types included PV and NPV, with die-off patches having higher NPV (litter and senescent vegetation) and much lower PV (green foliage). The combination of springtime PV and NPV fractions was sufficient to spectrally distinguish die-off and non-die-off cover types (Fig. 2). Shrub-dominated land-cover types had higher shade cover, lower NPV cover, and higher soil cover compared to either cheatgrass or die-off land-cover types.

The Random Forests algorithm, a machine learning approach that uses an ensemble of classification trees, was used to predict the probability of each pixel being “cheatgrass die-off” or “non-cheatgrass die-off” based upon spectral properties of the pixel, as defined using SMA from spring and summer Landsat imagery. The Random Forests method uses bootstrap samples to construct a large number of classification or regression trees (Breiman, 2001). Random Forests has been shown to perform better than single classification trees, can handle non-linear relationships, does not require data to be normally distributed, has methods for balancing error in unbalanced datasets, and has been used in a wide variety of remote sensing applications (Pal, 2005). The Random Forests model generates probabilities of occurrence of each pixel for each of the cover types. To generate a binary map of

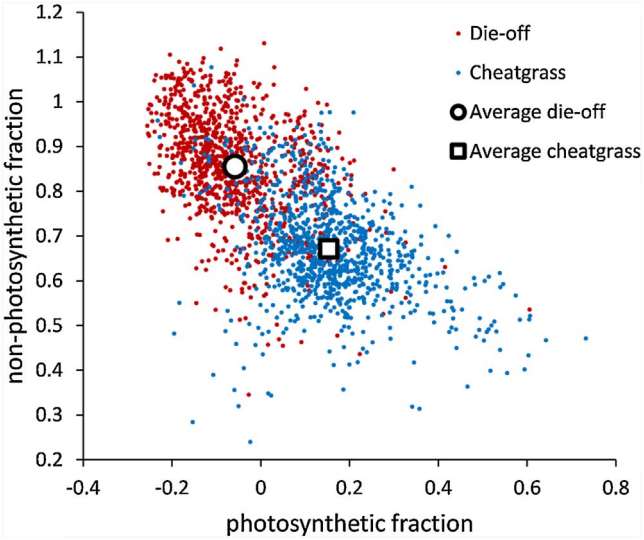

Fig. 2. Scatterplot showing separation of die-off and cheatgrass monoculture points along axes of photosynthetic and non-photosynthetic vegetation cover at based on random points located within and adjacent to photo-interpreted die-off polygons derived from May 22, 2014 Landsat (n = 1856). The spectral mixture analysis constrains the fraction of the four endmembers to equal 100% (unit sum constraint), but allows for negative fraction in cases where pixels are more pure than the endmembers themselves (overflow fractions).

die-off events and non-die-offs we used a probability threshold of 0.7. This threshold best minimized total error and best balanced errors of omission and errors of commission, based on the photo-interpreted die-off polygons from 2014 Landsat imagery.

Random points from within and adjacent to the photo-interpreted die-off polygons from May 22, 2014 Landsat imagery were used to train the Random Forests models. A Landsat scene from May 9, 2009, also a year with extensive amounts of die-off, was used to independently validate the models. We identified 381 die-off and 694 non-die-off points using the Landsat false-color composite from the spring of 2009. We calculated total agreement, omission error (false positives), and commission error (false negatives), and Cohen's kappa to estimate error in our die-off classification.

Mapped die-off polygons were assessed visually using a combination of Landsat imagery and 2013 National Agriculture Imagery Program (NAIP) aerial photographs to determine if the mapped patterns were real. To reduce the number of false positives, we omitted die-off polygons if they occurred in areas with low PV and were unlikely to have supported cheatgrass at any time during the 30 year time period. A threshold of 0.2 maximum PV cover throughout the 30 year time period was used to separate real die-off events from false positives. The 0.2 threshold was chosen because it served as a natural break that clearly separated a bimodal distribution of PV values that had peaks near 0.03 and 0.6.

2.4. Data analysis

Three levels of cheatgrass die-off were considered. The first level ("overall die-off") included all pixels classified as die-off from the spectral mixture analysis of Landsat imagery, as previously described. The second level ("persistent die-off") included only die-off pixels that were repeated in at least two consecutive years. The persistent die-off classification included adjacent pixels to allow for possible positional error in Landsat imagery, hence it included pixels that had die-off in only one consecutive year where a neighboring pixel had die-off in either the prior or following year. Finally, the third level ("hotspot die-off") incorporated only die-off events that occurred on pixels that experienced at least 4 die-off events over the 31-year record (≥13% prevalence), and that were available for recording die-off (i.e. not obscured by clouds) for at least 27 of the 31 years.

Spearman's rank correlations and scatter plots were used to relate die-off area in a given year with annual climate variables. Climate variables were quantified using weather data from the Winnemucca airport, and included current-year and lagged precipitation data (annual; winter = Oct–Mar; spring = Apr–May), temperature data (annual minimum and maximum; April maximum, May maximum), and climatic water deficit (the unmet evaporative demand for water by vegetation in a given year, a measure of drought stress) as calculated in Dilts et al. (2015). Multiple regression analysis was not used for final analysis because, in initial analyses, the most parsimonious models for each of the three die-off types included only a single predictor variable, based upon model comparisons using AICc statistics. Nonparametric Spearman's correlations were used because relationships between die-off and climate were highly nonlinear.

3. Results

3.1. Remote sensing methodology

The independent validation of the model developed for 2014 training data showed high classification success of die-off patches when applied to 2009 imagery, based upon a data set of 1075 photo-interpreted pixels (93% overall classification accuracy; Table 1). Error of omission for die-off pixels (13%) was comparable to error of commission (7%), indicating a relatively unbiased classification model. The corresponding kappa coefficient (κ) of 0.845 (95% CI: 0.812–0.879) indicates very good agreement relative to the frequency of correctly classified pixels expected by random chance. Field visitation in 2015 identified 12 of 13 areas mapped as die-off polygons (92%) as correctly classified. The post-classification removal of pixels having PV < 0.2 resulted in the removal of 3.8% of pixels incorrectly classified as die-off, further improving the accuracy of the model.

3.2. Cheatgrass die-off prevalence and interannual variability

Cheatgrass die-off extent has varied greatly from year to year (Fig. 3a), with a complete absence of die-off observed in certain years (2001, 2002, 2008), and extensive occurrence in others. For example, die-off was observed in nearly 2817 km^2 (4.1% of non-excluded portion of study area) in 2003, with the years 1990 and 2009 also experiencing relatively extensive areas of die-off (1262 km^2 and 652 km^2, respectively). Very little die-off was observed during two longer periods from 1993 to 1999, and from 2005 to 2008.

Periods with large areas of persistent die-off occurred from 1990 to 1991, 2003 to 2004, 2009 to 2010, and 2014 to 2015 (Fig. 3b). Although the year 2003 had the largest area of die-off, much of this die-off was ephemeral: only 11.7 km^2 of the 2817 km^2 die-off observed in that year proved to be persistent. The area of persistent die-off was nearly an order of magnitude lower than the area of die-off overall (Fig. 3a and b).

Areas classified as hotspots for die-off, where die-off occurred for at least 4 years of the 31-year record, occupied just 156.6 km^2, or 0.9% of the unmasked portion of the study area (Table 2). There was also considerable interannual variability in die-off occurrence in hotspot

Table 1
Confusion matrix for the 2014 Random Forests model applied to 2009, assuming a probability threshold of 0.7 to indicate die-off pixels. Presence of die-off and non-die-off was determined by photointerpretation of high-resolution imagery. The overall classification error of 0.07 corresponds to a classification accuracy of 0.93.

Photo-mapped	Die-off	Non-die-off	Omission Error
Die-off	331	50	0.13
Non-die-off	25	669	0.04
Commission Error	0.07	0.07	0.07

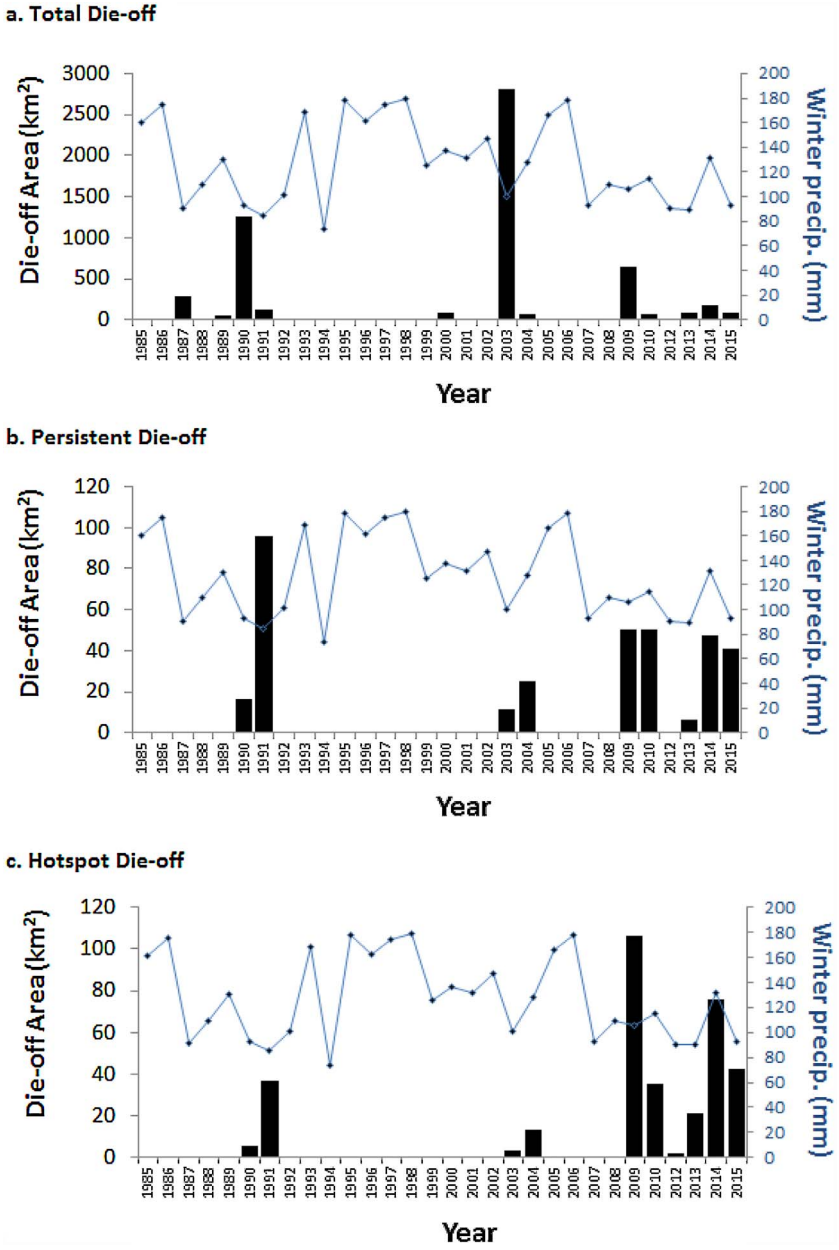

Fig. 3. Annual area of cheatgrass die-off recorded from 1985 to 2015, for (a) all patches classified as die-off; (b) patches classified as persistent die-off; and (c) patches classified as hotspot die-off. Also shown is winter precipitation (mm) as recorded at the Winnemucca airport. Vertical columns represent the extent of die-offs; line graphs represent winter precipitation.

Table 2
Frequency of die-off years recorded in cheatgrass die-off hotspot areas. Proportional areas are calculated based on the unmasked portion of the study area.

No. Events	Die-off Area (km^2)	Proportion of unmasked study area
4	105.81	0.0061
5	36.28	0.0021
6	10.10	0.0006
7	4.15	0.0002
8	0.20	< 0.0001
9	0.02	< 0.0001

areas (Fig. 3c). Die-off in hotspot areas was absent or limited in occurrence during 1985–1989, 1992–2002, and 2004–2009, but has become more prevalent since approximately 2009.

The complete time series of cheatgrass die-off maps is given in Supplementary materials, Fig. S-1.

3.3. Die-off relationships with climate

Interannual variability of all three die-off classifications was associated with drought indicators, particularly winter precipitation (moderate correlations with all three), the sum of annual precipitation in the preceding three years (especially for persistent die-off), the sum of winter precipitation for the preceding three years (especially for persistent and hotspot die-off), and springtime maximum temperature (especially for hotspot die-off). Correlations were negative for precipitation variables and weak for temperature and water deficit variables (Table 3). Strongest negative associations were with winter precipitation of the current water year and lagged annual precipitation from two or even three years prior, suggesting that widespread die-off events (including persistent and hotspot die-off) have been associated with winter drought that follows multiple years of low precipitation (a pattern evident in Fig. 3).

Relationships between climate variables and die-off were highly nonlinear (Fig. 4). Growing seasons following wet winters or wet

Table 3
Spearman's rank correlations of annual die-off area for the three cheatgrass die-off categories with selected climate variables from the Winnemucca weather station, summarized over 1985–2015 (n = 31 years). MaxT = mean monthly maximum temperature; MinT = mean monthly minimum temperature; CWD = climatic water deficit; WPrecip = winter precipitation (Oct–Mar); SprPrecip = spring precipitation (Apr–May); AprMaxT = April maximum temperature; MayMaxT = May maximum temperature; MAPpre = annual precipitation of the year prior; MAP2yr = summed precipitation of two years prior; MAP3yr = summed precipitation of three years prior; WPPTpre = winter precipitation of the year prior; WPPT2yr = summed winter precipitation of two years prior; WPPT3yr = summed winter precipitation of three years prior. Correlations > |0.4| are shown in bold font, with * indicating significance at $\alpha \leq 0.05$.

	Die-off	Persistent Die-off	Hotspot Die-off
MaxT	−0.06	−0.05	−0.06
MinT	0.13	0.22	0.26*
CWD	0.16	0.18	0.18
WPrecip	**−0.49***	**−0.48***	**−0.41***
SprPrecip	0.12	0.09	0.05
AprMaxT	0.15	0.21	0.22
MayMaxT	−0.04	−0.06	−0.01
MAPpre	−0.37*	−0.30	−0.35
MAP2yr	**−0.47***	**−0.56***	**−0.56***
MAP3yr	−0.27	**−0.50***	**−0.48***
WPPTpre	−0.05	−0.37	**−0.45***
WPPT2yr	−0.23	**−0.43***	**−0.51***
WPPT3yr	−0.26	**−0.45***	**−0.50***

sequences of preceding years never had large areas of die-off, whereas drought years below a certain threshold level of precipitation sometimes experienced extensive die-off, but did not always.

3.4. Die-off distribution and spatial pattern

Landsat pixels with cheatgrass die-off showed strong clustering within several low-lying areas including Dun Glen Valley and surroundings, Grass Valley, Eden and Paradise Valleys, a large patch near the Humboldt and Lander County boundaries north of Battle Mountain, and the eastern and western edges of the Quinn River Valley (Fig. 5a). Unsurprisingly, these same areas are reflected in the distribution of persistent die-off events, and of die-off hot spot areas (Fig. 5b and c). These results suggest that die-off events are strongly clustered and persistent within the same general locations, although more detailed examination of die-off occurrence from one year to the next shows that die-off patches have tended to shift spatially at fine spatial scales.

Most hotspot areas had already experienced die-off by early in the Landsat chronology (1980s), although die-off occurred in new parts of the study area during the widespread events of 2003 and 2009 (Fig. 5d). Recent die-off over the past 5 years has generally recurred in previous die-off areas.

The frequency distribution of die-off events of different sizes was strongly skewed (Fig. 6). Over 65% of die-off patches occupied less than 1 ha in area. Most patches (60%) were between 0.4 ha and 1 ha, with only 5.0% occupying less than 0.4 ha. Approximately 4.5% of die-off patches were larger than 10 ha, and the largest patch occupied 9819 ha (nearly 38 square miles).

3.5. Die-off duration

Die-off duration was strongly skewed towards single-year die-off events (81.5% of events), even in hotspot areas. Die-off of two- and three-year duration occurred for 18.2% and 0.4% of events, respectively. Die-off was often present in the same valley-bottom hotspot areas for longer time periods, but tended to shift to nearby patches over fine spatial scales. Die-off within a given patch was most likely to end during years of increasing (but not necessarily high) winter precipitation levels, including 1988, 1991, 2004 and 2010.

4. Discussion

The rangeland economy of the western U.S. has been severely damaged by the introduction of cheatgrass (DiTomaso, 2000; Pimentel et al., 2005), and this invasive annual grass is predicted to expand its distribution still further given regional climate change scenarios (Bradley, 2009; Creutzburg et al., 2015). Given its extreme impacts in the arid west, attempts to understand the extent and causes of the naturally-occurring die-off phenomenon are of high utility for land management in this region. The overall methodological approach can

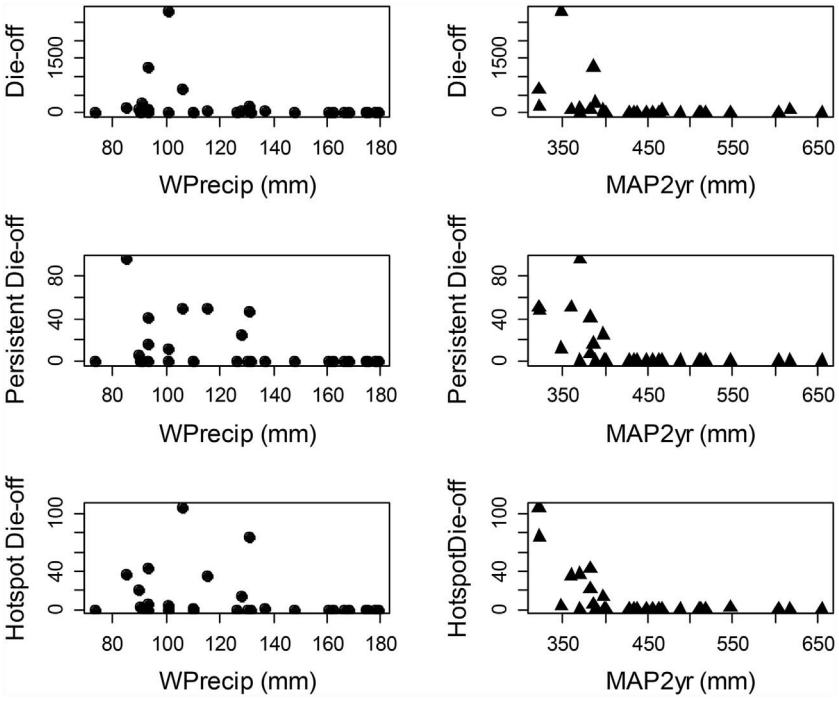

Fig. 4. Relationships between the three die-off categories with annual climate variables winter precipitation (WPrecip) and annual precipitation of the preceding two years (MAP2yr). Die-off areal units are in km^2; precipitation units are mm. Each observation refers to an individual year from 1985 to 2015 (n = 31).

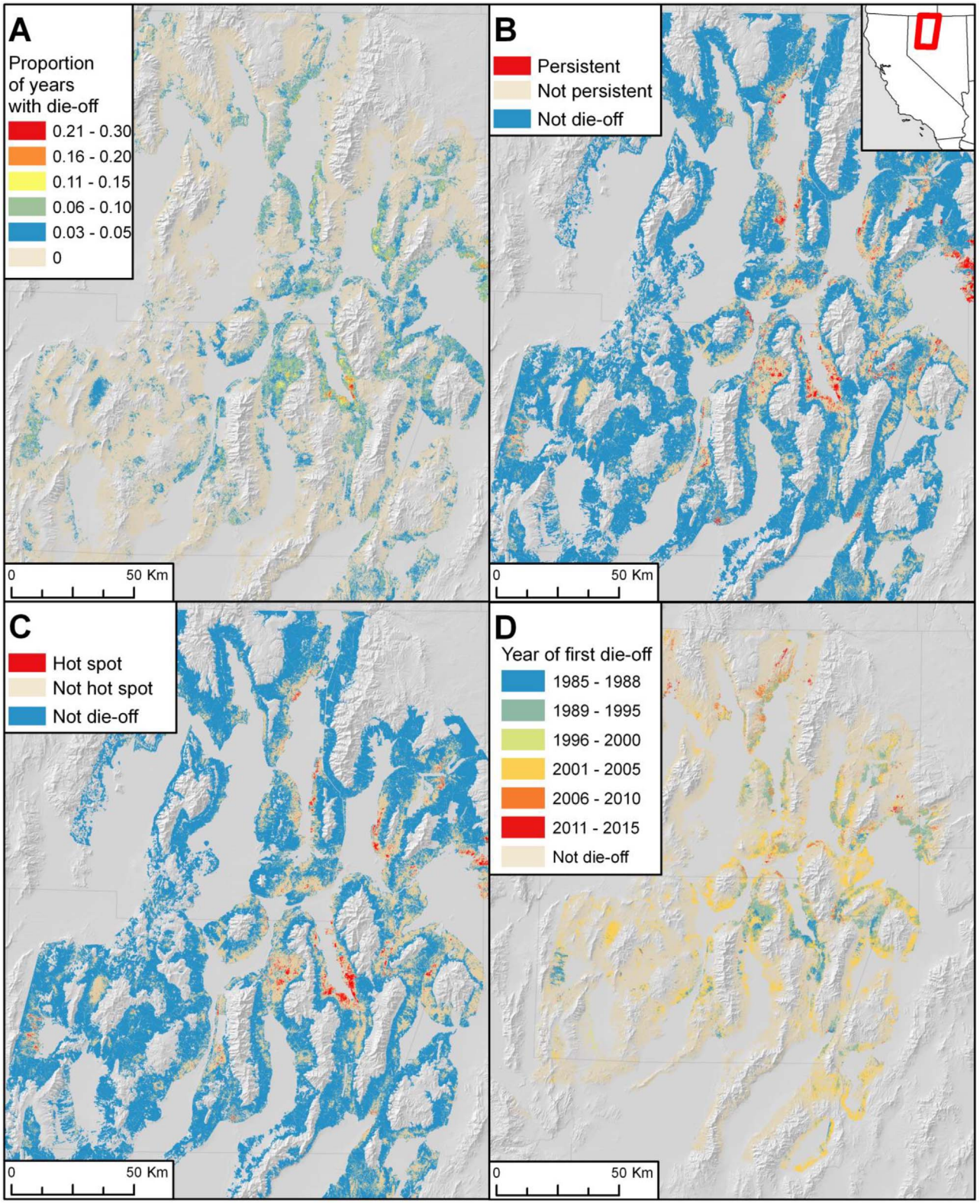

Fig. 5. A) Proportion of years in the 30 year time period experiencing die-off. B) Distribution of areas that have experienced persistent cheatgrass die-off, die-off that has not been persistent (i.e. ≥2 years of consecutive die-off), and an absence of die-off. C) Distribution of hotspot die-off areas that have experienced cheatgrass die-off for at least 4 years over the 1985–2015 period. D) Year of first die-off occurrence.

be extended to similar systems worldwide where it would be useful to map regeneration dynamics of annual grasslands over large regions. Here, we have demonstrated a novel method for detecting, classifying and mapping cheatgrass die-off patches using archival Landsat imagery that can be used to reconstruct historical die-off since 1985, as well as to model contemporary die-off. Our model obtained high accuracy against both field and photo-interpreted data that were not used to develop the classification (i.e. independent data). Because our approach relies solely on springtime imagery it can be applied to map current year's die-off within weeks after peak cheatgrass greenness in the

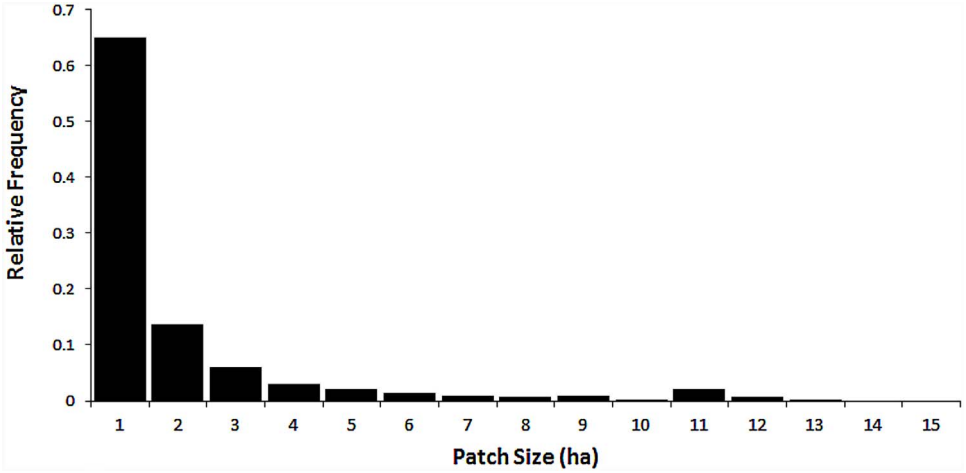

Fig. 6. Frequency distribution of patch sizes for die-off occurrences (n = 32,767) over the entire (1985–2015) period of record. The x-axis has been truncated to 15-ha although a small proportion (< 0.008) of patches exceeded that size.

spring, depending mainly on the date of cloud-free Landsat image collection, the interval until imagery is made available, and the short time needed for image processing and accuracy checking.

Our approach differs from other approaches that have emphasized the unique phenology of cheatgrass (i.e. the contrast in vegetation greenness between spring and summer; Peterson, 2005; Singh and Glenn, 2009), or else have focused on the strong sensitivity of cheatgrass to interannual variability in precipitation (e.g. Boyte et al., 2015; Bradley and Mustard, 2005, 2006; Clinton et al., 2010). The spectral mixture analysis methodology we have developed is not based upon the intra-annual or inter-annual dynamics of cheatgrass, but utilizes the unique characteristics of die-off patches themselves: massive amounts of litter in spring that persist through the summer months, with very little photosynthetic vegetation (particularly in spring), and low amounts of exposed soil or shadow. However, it is possible that our classification has reduced ability to detect older die-off patches that may no longer have a significant surface litter component; if so, this may be reflected in our analysis demonstrating that most die-offs persist for one year or less. Further field validation could be conducted to elucidate this issue.

Our results are likely scale-dependent given that the methodology is based upon a single source of imagery with 30-m pixel resolution (900 m^2 or 0.09-ha). Patch area calculations are strongly influenced by the pixel size used, as is our ability to resolve complex boundary shapes of die-off patches. Remote sensing studies using higher-resolution imagery would likely find a greater frequency of even smaller patches, whereas studies using coarse-resolution imagery (such as MODIS) would report larger patch sizes, but fail to detect die-off areas with a low density of small patches (e.g. < 1 ha). Multi-resolution mapping of die-off (e.g. fusing high-resolution satellite or UAV imagery with Landsat and MODIS data) would be desirable for combining the need to accurately map small patches for restoration purposes, with the ability to map die-off over the sufficiently large areas of management concern. Finally, although our remote sensing methodology was developed for a large region of varying cheatgrass cover, soil type and productivity, its generalizability to larger scales (e.g. the extent of cheatgrass distribution within its invaded range in western North America) would be improved through application and calibration to different study areas and environmental conditions.

4.1. Implications of observed spatiotemporal dynamics for inferring die-off causes

The causal mechanisms behind the die-off phenomenon are still incompletely understood. They appear to involve interactions of at least three soilborne fungal pathogens with each other and with patterns of litter persistence as well as with inter-annual weather variation (Franke et al., 2014a,b; Meyer et al., 2014, 2016). Here, we assess the inferential support for mechanisms underlying cheatgrass die-off from observed patterns of occurrence as reconstructed from a 31-year Landsat archive.

Previous field-based investigations from scattered locations have noted that cheatgrass die-offs are transient phenomena, typically returning to cheatgrass monocultures within one or a few years (Baughman and Meyer, 2013). Soilborne pathogens directly associated with die-off events do not appear to affect the persistent seed bank or to prevent cheatgrass recruitment in subsequent years, allowing usually rapid stand recovery in this annual grass. Our results support the generalizability of this finding across a large continuous landscape, where the great majority of die-off events lasted for a single year. Following die-off, cheatgrass can re-establish from the in situ seed-bank or, in the absence of a seed bank, by much slower colonization from outside the patch, leading to a more persistent die-off scenario.

There may be strong feedbacks between cheatgrass dominance and die-off occurrence that lead to an oscillating cycle, mediated by conditions of heavy litter that predispose a site to pathogenically induced die-off, as proposed by Baughman and Meyer (2013). This could lead to the pattern of recurrent die-off that was sometimes observed (die-off hotspots).

We found a strong correspondence between die-off events and winter drought conditions, observing strongest negative associations of die-off with current year winter precipitation and previous years' lagged winter and annual precipitation. This finding, manifest across our 60,000 km^2 study area, mirrors results from controlled experiments where water potential was manipulated to determine how environmental conditions influenced susceptibility of cheatgrass seeds to the *Fusarium* seed rot pathogen (Meyer et al., 2014). Meyer et al. (2014) found that emergence failure associated with *Fusarium* was greatest following conditions of water stress; at high water availability seed pathogens were disadvantaged by rapid rates of seed germination. Because *Fusarium* populations remain active at soil water availability levels far below those needed for cheatgrass seed germination (Woods and Duniway, 1986), *Fusarium* may be capable of exerting strong control on cheatgrass emergence during dry years with limited and intermittent precipitation during the fall/early spring germination window. *Fusarium* species are ubiquitous in the soils underlying cheatgrass monocultures, but their ability to cause epidemic disease is likely related to pathogen load and soil carbon dynamics as well as soil moisture (Meyer et al., 2016).

Despite the apparently strong controls of regional-scale climate

variability on die-off occurrence, the observed tight spatial clustering of persistent and hotspot die-off patches, within areas that otherwise appear to be fairly homogeneous in topography and soil type, suggests strong pathogen limitation. Taken together, the spatiotemporal patterns of cheatgrass die-off quantified through our classification of the Landsat archive suggest that climate sets the stage for die-off, but that other limiting conditions must also be overcome. Such conditions could be related to litter accumulation (Baughman and Meyer, 2013) or critical levels of fungal pathogen populations. Remote sensing indicators are needed, in combination with field and laboratory experiments, to develop a predictive understanding of landscape-level, pathogen-induced phenomena (such as cheatgrass die-off) that depend on spatial population dynamics of both host and pathogen, as these interact with the abiotic environment across heterogeneous landscapes (Holdenrieder et al., 2004). Such predictive models would further support ecological restoration applications including reseeding or planting of desired native species into cheatgrass die-off areas, and identification of where mitigation practices are required for ameliorating the undesirable consequences of die-off such as wind erosion.

Acknowledgments

This work was funded by the Bureau of Land Management under the Integrated Cheatgrass Die-off Project, as well as by the Great Basin Landscape Conservation Cooperative (2013). Aaron Coogan, Elana Ketchian, and Emma Verberne assisted with image processing.

Appendix A. Supplementary data

Supplementary data associated with this article can be found, in the online version, at http://dx.doi.org/10.1016/j.ecolind.2017.04.024.

References

Balch, J.K., Bradley, B.A., D'Antonio, C.M., Gómez-Dans, J., 2013. Introduced annual grass increases regional fire activity across the arid western USA (1980–2009). Glob. Change Biol. 19, 173–183.
Baughman, O.W., Meyer, S.E., 2013. Is *Pyrenophora semeniperda* the cause of downy brome (*Bromus tectorum*) die-offs? Invasive Plant Sci. Manage. 6, 173–183.
Baughman, O.W., Meyer, S.E., Aanderud, Z.T., Leger, E.A., 2016. Cheatgrass die-offs as an opportunity for restoration in the Great Basin, USA: Will local or commercial native plants succeed where exotic invaders fail? J. Arid Environ. 124, 193–204.
Blank, R., Morgan, T., Clements, D., 2011. Cheatgrass dead zones in northern Nevada. Proc. Soc. Range Manage. 64, 94.
Boyte, S.P., Wylie, B.K., Major, D.J., 2015. Mapping and monitoring cheatgrass dieoff in rangelands of the Northern Great Basin, USA. Rangeland Ecol. Manage. 68, 18–28.
Bradley, B.A., Fleishman, E., 2008. Relationships between expanding pinyon-juniper cover and topography in the central Great Basin, Nevada. J. Biogeogr. 35, 951–964.
Bradley, B.A., Mustard, J.F., 2005. Identifying land cover variability distinct from land cover change: cheatgrass in the Great Basin. Remote Sens. Environ. 94, 204–213.
Bradley, B.A., Mustard, J.F., 2006. Characterizing the landscape dynamics of an invasive plant and risk of invasion using remote sensing. Ecol. Appl. 16, 1132–1147.
Bradley, B.A., 2009. Regional analysis of the impacts of climate change on cheatgrass invasion shows potential risk and opportunity. Glob. Change Biol. 15, 196–208.
Breiman, L., 2001. Random forests. Mach. Learn. 45, 5–32.
Chander, G., Markham, B.L., Helder, D.L., 2009. Summary of current radiometric calibration coefficients for Landsat MSS, TM, ETM+, and EO-1 ALI sensors. Remote Sens. Environ. 113, 893–903.
Clinton, N.E., Potter, C., Crabtree, B., Genovese, V., Gross, P., Gong, P., 2010. Remote sensing-based time-series analysis of cheatgrass (L.) phenology. J. Environ. Qual. 39, 955–963.
Creutzburg, M.K., Halofsky, J.E., Halofsky, J.S., Christopher, T.A., 2015. Climate change and land management in the rangelands of central Oregon. Environ. Manage. 55, 43–55.
D'Antonio, C.M., Vitousek, P.M., 1992. Biological invasions by exotic grasses, the grass/fire cycle, and global change. Annu. Rev. Ecol. Syst. 23, 63–87.
DiTomaso, J.M., 2000. Invasive weeds in rangelands: species, impacts, and management. Weed Sci. 48, 255–265.
Dilts, T.E., Weisberg, P.J., Dencker, C.M., Chambers, J.C., 2015. Functionally relevant climate variables for arid lands: a climatic water deficit approach for modelling desert shrub distributions. J. Biogeogr. 42, 1986–1997.
Duncan, C.A., Jachetta, J.J., Brown, M.L., Vanelle, F.C., Clark, J.K., DiTomaso, J.M., Lym, R.G., McDaniel, K.C., Renz, M.J., Rice, P.M., 2004. Assessing the economic, environmental, and societal losses from invasive plants on rangeland and wildlands. Weed Technol. 18, 1411–1416.
Elmore, A.J., Mustard, J.F., Manning, S.J., Lobell, D.B., 2000. Quantifying vegetation change in semiarid environments: precision and accuracy of spectral mixture analysis and the normalized difference vegetation index. Remote Sens. Environ. 73, 87–102.
Esri (Environmental Systems Research Institute), 2012. ArcGIS Desktop version 10.1. Redlands, CA.
Exelis Visual Information Solutions, 2012. ENvironment for Visualizing Images (ENVI) version 4.8. Boulder, CO.
Franke, J., Geary, B., Meyer, S.E., 2014a. Identification of the infection route of a *Fusarium* seed pathogen into nondormant *Bromus tectorum* seeds. Phytopathology 104, 1306–1313.
Franke, J., Meyer, S.E., Geary, B., 2014b. Bleach blonde syndrome, a new disease of *Bromus tectorum* implicated in cheatgrass die-offs. Abstract. Botanical Society of America, Botany 2014, July 26–30, 2014m, Boise, Idaho. http://2014.botanyconference.org/engine/search/index.php?func=detail&aid=446.
Greenwood, D.L., Weisberg, P.J., 2009. GIS-based modeling of pinyon-juniper woodland structure in the Great Basin. For. Sci. 55, 1–12.
Holdenrieder, O., Pautasso, M., Weisberg, P.J., Lonsdale, D., 2004. Tree diseases and landscape processes: the challenge of landscape pathology. Trends Ecol. Evol. 19, 446–452.
Humphrey, L.D., Schupp, E.W., 2004. Competition as a barrier to establishment of a native perennial grass (*Elymus elymoides*) in alien annual grass (*Bromus tectorum*) communities. J. Arid Environ. 58, 405–422.
Mack, R.N., 1981. Invasion of *Bromus tectorum* L. into western North America: an ecological chronicle. Agroecosystems 7, 145–165.
Meyer, P., Itten, K.I., Kellenberger, T., Sandmeier, S., Sandmeier, R., 1993. Radiometric corrections of topographically induced effects on Landsat TM data in an alpine environment. ISPRS J. Photogramm. 48, 17–28.
Meyer, S.E., Franke, J.L., Baughman, O.W., Beckstead, J., Geary, B., 2014. Does *Fusarium*-caused seed mortality contribute to *Bromus tectorum* stand failure in the Great Basin? Weed Res. 54, 511–519.
Meyer, S.E., Beckstead, J., Pearce, J.L., 2016. Community ecology of fungal pathogens on *Bromus tectorum*. In: Chambers, J., Germino, M., Brown, C. (Eds.), Exotic Annual *Bromus* Grasses in Semiarid Ecosystems of the Western US: Assessing Causes, Consequences, and Management Alternatives. Springer Verlag.
Pal, M., 2005. Random forest classifier for remote sensing classification. Int. J. Remote Sens. 26, 217–222.
Peterson, E.B., 2005. Estimating cover of an invasive grass (*Bromus tectorum*) using tobit regression and phenology derived from two dates of Landsat ETM+ data. Int. J. Remote Sens. 26, 2491–2507.
Pimentel, D., Zuniga, R., Morrison, D., 2005. Update on the environmental and economic costs associated with alien-invasive species in the United States. Ecol. Econ. 52, 273–288.
Rafferty, D.L., Young, J.A., 2002. Cheatgrass competition and establishment of desert needlegrass seedlings. J. Range Manage. 55, 70–72.
Rowe, C.L.J., Leger, E.A., 2011. Competitive seedlings and inherited traits: a test of rapid evolution of *Elymus multisetus* (big squirreltail) in response to cheatgrass invasion. Evol. Appl. 4, 485–498.
Salo, C., 2011. Land lines: the cheatgrass that wasn't there. Rangelands 33, 60–62.
Singh, N., Glenn, N.F., 2009. Multitemporal spectral analysis for cheatgrass (*Bromus tectorum*) classification. Int. J. Remote Sens. 30, 3441–3462.
Woods, D.M., Duniway, J.M., 1986. Some effects of water potential on growth, turgor, and respiration of *Phytophthora cryptoge*a and *Fusarium moniliforme*. Phytopathology 76, 1248–1254.
Yang, J., Weisberg, P.J., Bristow, N.A., 2012. Landsat remote sensing approaches for monitoring long-term tree cover dynamics in semi-arid woodlands: comparison of vegetation indices and spectral mixture analysis. Remote Sens. Environ. 119, 62–71.
Young, J.A., Evans, R.A., 1978. Population dynamics after wildfires in sagebrush grasslands. J. Range Manage. 31, 283–289.
Zhu, Z., Woodcock, C.E., Olofsson, P., 2012. Continuous monitoring of forest disturbance using all available Landsat imagery. Remote Sens. Environ. 122, 75–91.